Compact Microstrip Bandpass Filters With Good Selectivity and Stopband Rejection

Pu-Hua Deng, Yo-Shen Lin, *Member, IEEE*, Chi-Hsueh Wang, and Chun Hsiung Chen, *Fellow, IEEE*

Abstract—**Compact microstrip bandpass filters (second- and fourth-order) are proposed based on the folded quarter-wavelength ($\lambda/4$) resonators, which are mainly coupled through the shunt inductors connected to the ground. By introducing a cross-coupling capacitance directly between the input and output ports of the second-order filter, a pair of transmission zeros may be created to improve the selectivity. Moreover, by an extension of the proposed second-order filter with the incorporation of an additional cross-coupling capacitance, a fourth-order filter is also proposed in which two pairs of transmission zeros may be created to improve both the selectivity and stopband rejection. The proposed fourth-order filter also has the merits of small circuit area and no spurious response up to $3f_0$, where f_0 is the passband center frequency. To provide effective design tools, simple equivalent-circuit models are also established.**

Index Terms—**Bandpass filter, cross-coupling, microstrip, quarter-wavelength resonators.**

I. INTRODUCTION

IN MICROWAVE communication systems, high-performance and small-size bandpass filters are required to enhance the system performance and to reduce the fabrication cost. Many microstrip filter structures using half-wavelength ($\lambda/2$) or quarter-wavelength ($\lambda/4$) resonators have been proposed. The conventional $\lambda/2$ resonator filters [1] have the drawback of a large circuit area. To solve this problem, the hairpin filter using folded $\lambda/2$ resonator structures [2]–[6] was developed. Thus, the circuit area may be reduced without degrading its performance. In addition, by introducing the cross-coupled effect in the hairpin resonator filter, one may create the transmission zeros [3]–[6] to improve the filter selectivity. In order to reduce interference by keeping out-band signals from reaching a sensitive receiver, a high-performance filter with wider upper stopband is also required. However, the planar bandpass filters made of $\lambda/2$ resonators inherently have the spurious passbands at multiple of the center frequency ($nf_0, n = 2, 3, \ldots$), which limit the rejection frequency range of the upper stopband.

By adopting the quarter-wavelength ($\lambda/4$) resonators, the filters may be made compact and may have good stopband rejection with the first spurious passband at three times the center frequency ($3f_0$) [7]–[13]. The interdigital [7]–[9] and combline [9] filters are two of the conventional reduced-size filters with $\lambda/4$ resonators. In [10] and [11], by using the folded $\lambda/4$ resonators, the interdigital and combline filters can be made more compact. In [10]–[12], the microstrip cross-coupled filters with electrical cross-coupling to create the transmission zeros were realized by bending the open end of $\lambda/4$ resonators. In [13], the stepped-impedance resonators were employed to implement the microstrip interdigital filter so that both size reduction and stopband extension may be achieved.

In our previous study [14], a compact second-order microstrip bandpass filter based on folded $\lambda/4$ resonators was proposed. The filter structure in [14] looks somewhat like the conventional combline filter [15], but their coupling mechanisms are different. Specifically, the resonators of [14] are mainly coupled through a shunt inductor connected to the ground, while the resonators of the combline filter are coupled through the parallel-coupled mechanism. In the filter structure of [14], a cross-coupling capacitance is introduced directed across the resonators so that two transmission zeros may be created for improving the stopband rejection, as the one did in the combline filter [10], [11]. However, the transmission zeros created in [14] are not near the passband edges, thus the filter selectivity is not good and needs improvement.

In this study, by alternatively introducing the cross-coupling capacitance directly between the input and output ports, one may achieve a different type of second-order microstrip bandpass filter for which the transmission zeros can be moved much closer to the center frequency (f_0) such that the selectivity can be improved. Moreover, by an extension of the proposed second-order filter with the incorporation of an additional cross-coupling capacitance, a fourth-order filter is also proposed, in which two pairs of transmission zeros may be created to improve both the selectivity and stopband rejection. Note that the proposed compact fourth-order microstrip bandpass filter exhibits the quasi-elliptic responses that may be produced by the conventional cascaded quadruplet (CQ) filters [4]–[7], [10]–[12]. To facilitate the filter design, simple equivalent-circuit models are also established.

II. SECOND-ORDER FILTER

In order to improve the selectivity of the filter in of the filter [14], a second-order microstrip bandpass filter structure composed of folded $\lambda/4$ resonators is proposed by placing the cross-coupling capacitor C_2 directly between the input and output
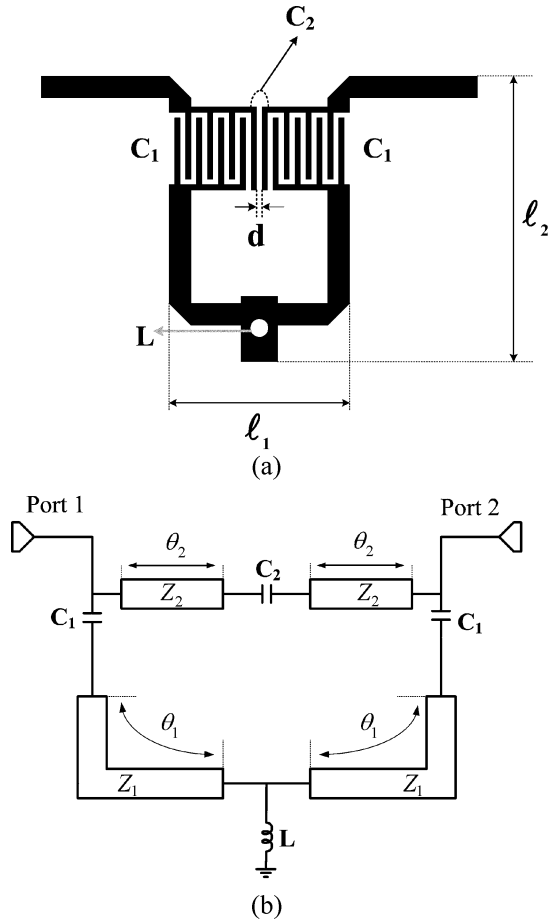
Fig. 1. Proposed second-order microstrip bandpass filter. (a) Layout. (b) Circuit model.
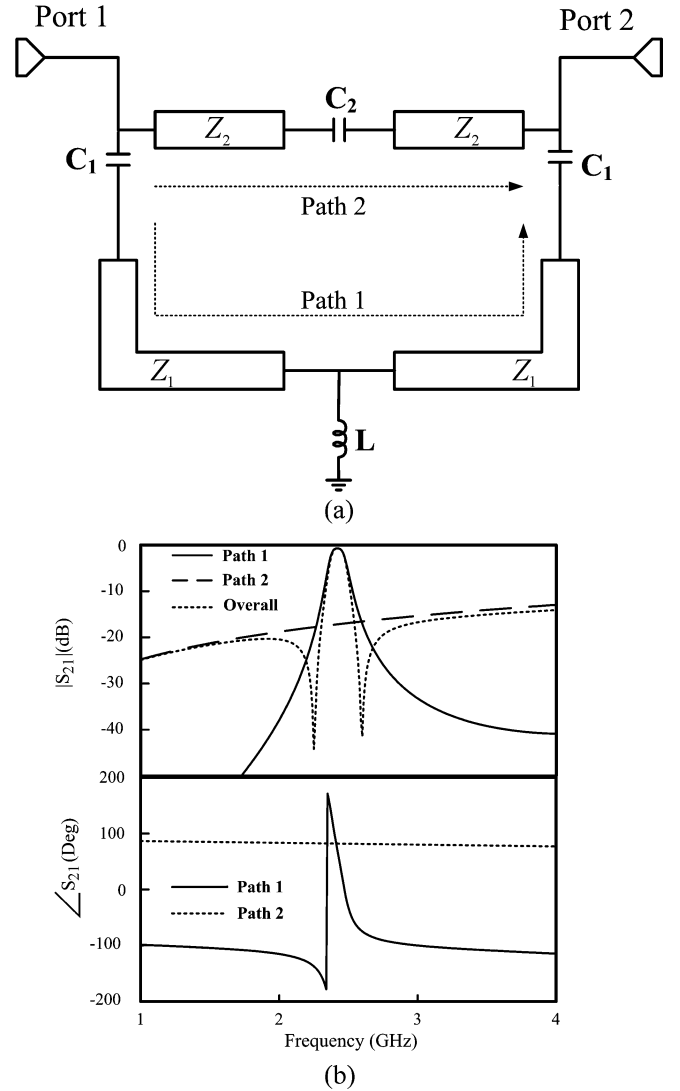

Fig. 2. (a) Two signal paths for the filter circuit model shown in Fig. 1(b). (b) Circuit-model simulated frequency responses of the two signal paths.

ports, as shown in Fig. 1(a). The two $\lambda/4$ resonators are mainly coupled through the shunt inductor L, which is realized by a metal via to the ground. The circuit model for the proposed filter is shown in Fig. 1(b). The design procedures for the proposed filter [see Fig. 1(a)] are almost the same as the ones in [14], except for the placement of C_2. Note that the folded resonators are utilized in the filter design for size reduction with the tradeoff of increasing the insertion loss in the passband.

For the filter structure shown in Fig. 1, the cross-coupling capacitor C_2 is used to create a pair of transmission zeros for improving the filter selectivity. The physics for creating the transmission zeros may be illustrated in Fig. 2. Here, the shunt inductor L provides the main signal path [path 1 in Fig. 2(a)] for the proposed filter circuit model [see Fig. 1(b)], while the capacitor C_2 introduces a second cross-coupling path (Path 2) along which the signal would cancel the one traveling along Path 1 at certain frequencies. Simulated frequency responses for this filter circuit model along Paths 1 and 2 [see Fig. 2(a)] are shown in Fig. 2(b). The signals from these two paths have the same amplitude and are nearly 180° out-of-phase at two frequencies such that they would cancel out each other at these two frequencies. Therefore, the overall filter response, also shown in Fig. 2(b), has two transmission zeros.

Typical simulated responses of the filter circuit model [see Fig. 1(b)] are shown in Fig. 3(a). This filter exhibits lower

and upper stopband transmission zeros, as expected. As C_2 increases, the transmission zeros move closer to f_0 at the expense of degrading the insertion loss in the stopband.

The transmission zeros of the proposed filter [see Fig. 1(a)] can also be discussed by the even- and odd-mode analyses of the circuit model in Fig. 1(b). Assuming that the proposed structure is symmetric, then the transfer function S_{21} may be related to the even- and odd-mode input impedances Z_{even} and Z_{odd} as

$$S_{21} = \frac{Z_1(Z_{\text{even}} - Z_{\text{odd}})}{(Z_{\text{even}} + Z_1)(Z_{\text{odd}} + Z_1)} \tag{1}$$

where

$$Z_{\text{even}} = \frac{Z_{Ae} \times Z_{Be}}{Z_{Ae} + Z_{Be}}$$

$$Z_{Ae} = \frac{Z_2}{j \tan \theta_2}$$

$$Z_{Be} = \frac{1}{j\omega C_1} + Z_1 \frac{j2\omega L + jZ_1 \tan \theta_1}{Z_1 + j \times 2\omega L \tan \theta_1} \tag{2}$$
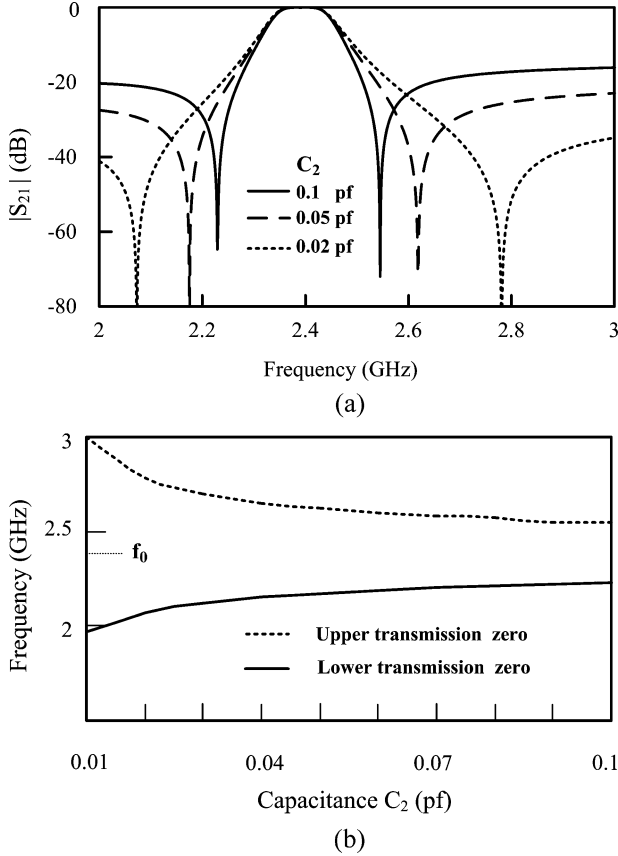
Fig. 3. (a) Simulated responses of the filter circuit model [see Fig. 1(b)] for various values of C_2. (b) Curves to relate the transmission-zero frequencies to the values of C_2. ($f_0 = 2.4$ GHz, $Z_1 = Z_2 = 50$ Ω, $\theta_1 = 79.4°$, $\theta_2 = 10°$, $C_1 = 0.23$ pF, $L = 0.092$ nH).

and

$$Z_{\text{odd}} = \frac{Z_{Ao} \times Z_{Bo}}{Z_{Ao} + Z_{Bo}}$$

$$Z_{Ao} = Z_2 \frac{\dfrac{1}{j2\omega C_2} + jZ_2 \tan \theta_2}{Z_2 + j \times \dfrac{1}{j2\omega C_2} \tan \theta_2}$$

$$Z_{Bo} = \frac{1}{j\omega C_1} + jZ_1 \tan \theta_1. \tag{3}$$

Here, Z_i and θ_i are the characteristic impedance and electrical length of the transmission line i ($i = 1$ for the main signal path, $i = 2$ for the cross-coupling path) and ω is the angular frequency. The transmission zeros are created when the transfer function in (1) becomes zero ($S_{21} = 0$), which implies

$$Z_{\text{even}} = Z_{\text{odd}}. \tag{4}$$

By using (4), one may obtain two solutions for ω, which correspond to the two transmission zeros at the upper and lower stopbands.

From (4), one can relate the frequencies of two transmission zeros to the values of the capacitance C_2. The specific curves for the cases center frequency $= 2.4$ GHz, $\theta_1 = 79.4°$, $\theta_2 = 10°$, $L = 0.092$ nH, $C_2 = 0.01$–0.1 pF are shown in Fig. 3(b). As the value of C_2 increases, the two transmission zeros will move

toward the center frequency f_0. Shown in Fig. 3(a) are the circuit-model simulated responses for various values of C_2 (0.02, 0.05, 0.1 pF) to demonstrate the influence of the transmission zeros on the insertion loss. When the value of C_2 increases, the upper and lower stopband transmission zeros will be close to the passband edges with the passband insertion loss essentially not degraded.

The proposed second-order bandpass filter structure (Fig. 1) is implemented using the microstrip configuration. In this study, all the circuits are fabricated on the Rogers RO4003C substrate ($\varepsilon_r = 3.38$, $\tan \delta = 0.002$, and thickness $h = 0.508$ mm). Shown in Fig. 1(a) is the layout of the proposed second-order microstrip bandpass filter based on the circuit model in Fig. 1(b).

The implemented filter is very compact and has a dimension of $0.13\lambda \times 0.18\lambda$ ($1_1 = 9.97$ mm, $1_2 = 13.7$ mm), where λ is the guided wavelength of the microstrip structure at the center frequency. This filter is designed according to the second-order maximally flat response with a center frequency of 2.4 GHz, a 3-dB bandwidth of 5.4%, and a reference impedance of 50 Ω. The required electrical length, capacitance C_1, and inductance L can be obtained based on the proposed equivalent-circuit model and the filter synthesis formulas [1]. Here, the shunt inductor L is realized by a metal-coated via to the ground. The diameter of the via and the length of pad are determined by the required inductance value. The capacitors C_1 and C_2 in Fig. 1(a) are implemented by the interdigital and gap structures, respectively. The value of C_2 is suitably chosen according to (4) to produce the desired locations of transmission zeros. The corresponding geometrical parameters are fine tuned in the full-wave simulator Ansoft Ensemble 8.0.

The measured and simulated results of the proposed filter [see Fig. 1(a)] are shown in Fig. 4. The measured center frequency is at 2.42 GHz, the minimum insertion loss is 1.82 dB at 2.42 GHz, and the 3-dB bandwidth is 5.5%. Good agreement between measured and simulated results is observed, except for a slight frequency shift of less than 1%. Two transmission zeros are found at 2.14 and 2.64 GHz. Note that, as expected, no repeated passband at $2f_0$ is observed.

The locations of the upper and lower stopband transmission zeros for the filter in Fig. 1(a) may simply be adjusted by controlling the gap-coupled capacitance C_2 through varying the gap spacing d. Shown in Fig. 5 are the measured results of the filter in Fig. 1(a) for various values of d. As C_2 increases by decreasing d, the two transmission zeros move toward the center frequency at the expense of degrading the stopband rejection. An even larger C_2 may be obtained by employing the interdigital capacitor to give the upper and the lower stopband transmission zeros closer to f_0. Note that the passband frequency responses remain almost unchanged as the value of C_2 is varied. This justifies the proposed design procedures and equivalent-circuit models in which the cross-coupling capacitance C_2 between the input and output ports is neglected first in the initial design stage and is then added back for creating the transmission zeros. Depending on the required falloff rate at passband edge and the level of stopband rejection, one may determine the required C_2 value and the locations of transmission zeros.
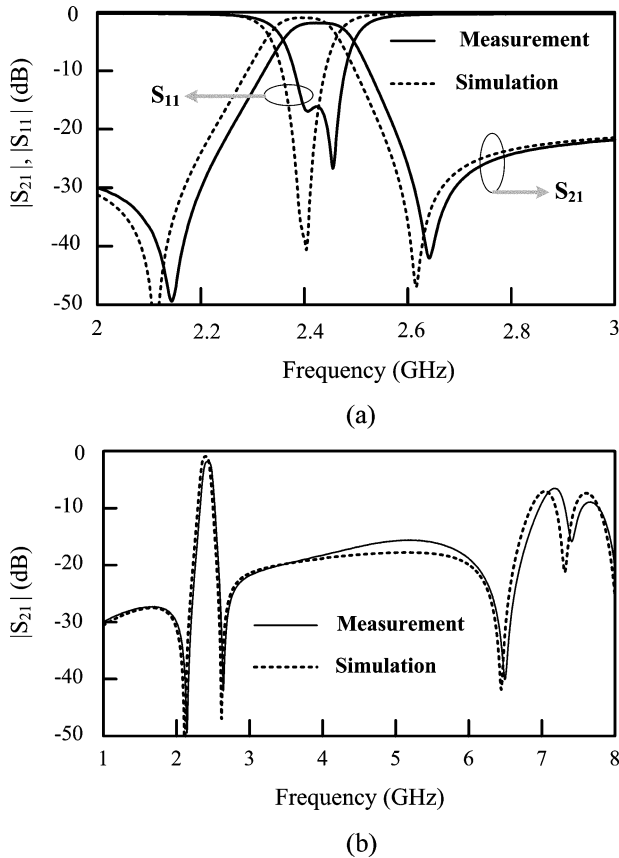
Fig. 4. Measured and simulated results of the proposed second-order microstrip filter in Fig. 1(a). (a) Narrow- and (b) wide-band frequency responses ($1_1 = 9.9$ mm, $1_2 = 15.65$ mm).
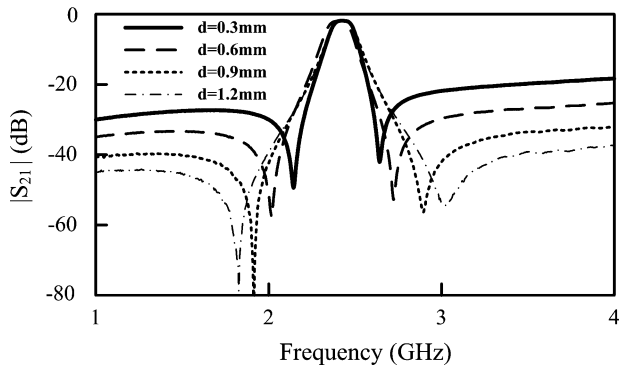

Fig. 5. Measured frequency responses of the second-order microstrip filter in Fig. 1(a) for various values of gapwidth d.

III. FOURTH-ORDER FILTER

By extending the cross-coupling mechanism in the second-order filter structure, a fourth-order bandpass filter with good selectivity, as well as improved stopband rejection may be built. The layout of the proposed fourth-order microstrip bandpass filter is shown in Fig. 6(a). Here, the capacitors C_1 and C_1' are implemented by the interdigital structures, and the capacitor C_2 is constructed by the gap configuration. Note that there is a very small coupling capacitance C_3 between the input and output ports, which may generate the transmission zeros far away from the passband.
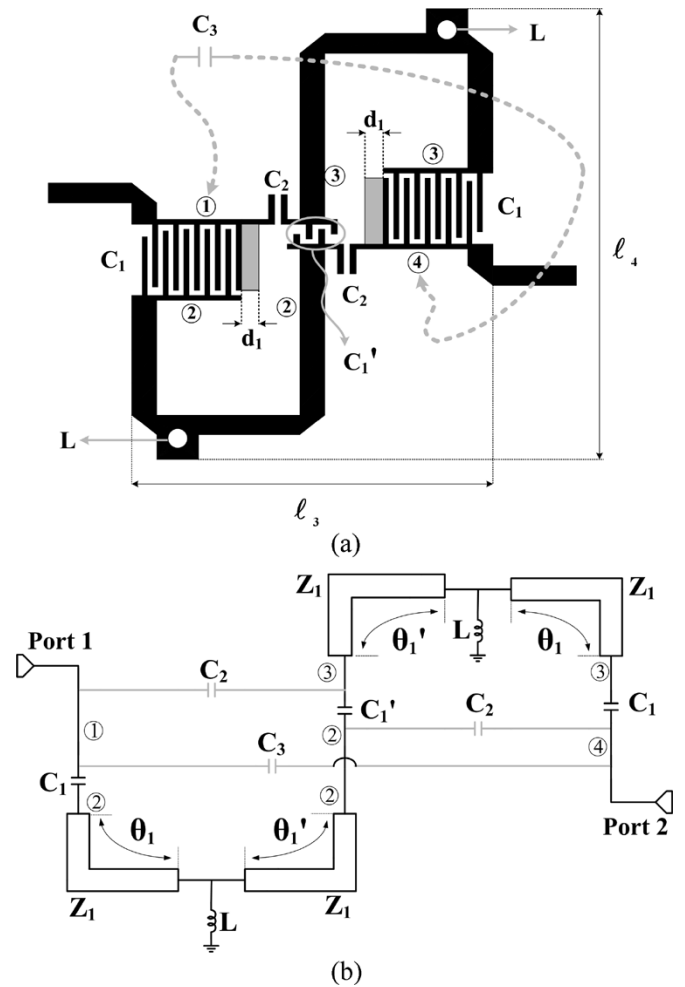

Fig. 6. Proposed fourth-order microstrip bandpass filter. (a) Layout. (b) Circuit model.

Shown in Fig. 6(b) is the equivalent-circuit model of the proposed fourth-order microstrip filter [see Fig. 6(a)], which has four folded $\lambda/4$ resonators. The capacitor C_1' and two capacitors C_1 along with proper lengths of transmission lines at their ends may be equivalent to three J-inverters. The two inductors L may be served as two K-inverters. Therefore, by neglecting the cross-coupling capacitances (C_2, C_3) in the circuit model [see Fig. 6(b)], the proposed filter is equivalent to a fourth-order bandpass filter. Based on the equivalent-circuit model, the design formulas for the proposed fourth-order microstrip filter may simply be obtained.

Note that the circuit model in Fig. 6(b) without the cross-coupling capacitance C_3 included is inadequate in predicting the response of the filter structure in Fig. 6(a). Specifically, with only C_2 being included in Fig. 6(b) (C_3 not included), the filter circuit model in Fig. 6(b) could only generate two transmission zeros near the passband edge. It is the combination of the cross-coupling mechanisms through both C_2 and C_3 that creates four transmission zeros, two of them near the passband edges and the other two far from the passband.

Basically, the cross-coupling capacitances C_2 are introduced in the fourth-order filter to create a pair of transmission zeros near the passband edges for improving the selectivity as the
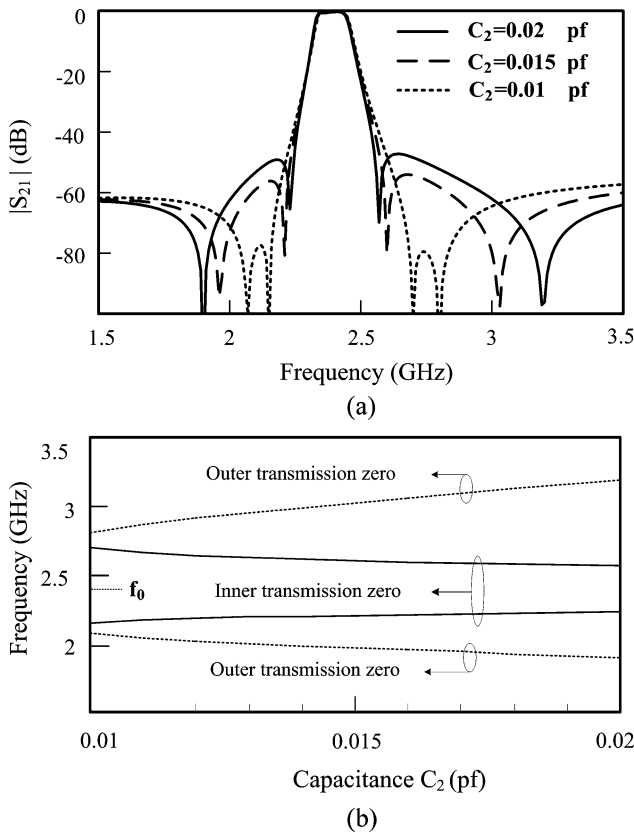
Fig. 7. (a) Simulated responses of the filter circuit model [see Fig. 6(b)] for various values of C_2. (b) Curves to relate the transmission-zero frequencies to the values of C_2 ($f_0 = 2.4$ GHz, $Z_1 = 50$ Ω, $\theta_1 = 75.4°$, $\theta_1' = 86.9°$, $L = 0.11$ nH, $C_1 = 0.316$ pF, $C_1' = 0.0279$ pF, $C_3 = 0.001$ pF).

Fig. 8. (a) Simulated responses of the filter circuit model [see Fig. 6(b)] for various values of C_3. (b) Curves to relate the transmission-zero frequencies to the values of C_3 ($f_0 = 2.4$ GHz, $Z_1 = 50$ Ω, $\theta_1 = 75.4°$, $\theta_1' = 86.9°$, $L = 0.11$ nH, $C_1 = 0.316$ pF, $C_1' = 0.0279$ pF, $C_2 = 0.0125$ pF).

second-order filter did. In order to further improve the stopband rejection, another cross-coupling capacitance C_3 directly between the input and output ports is introduced to generate an additional pair of transmission zeros far from the passband. The value of this cross-coupling capacitance C_3 is very small.

The simulated responses of the filter circuit model [see Fig. 6(b)] are shown in Figs. 7 and 8. Fig. 7(a) shows the corresponding circuit-model simulated responses for various values of C_2, and Fig. 7(b) relates the four transmission-zero frequencies to the values of C_2. As C_2 increases, the inner pair of transmission zeros (with respect to the passband center frequency f_0) will move toward the passband edges, while the outer pair of transmission zeros will move away from the passband, as demonstrated in Fig. 7(b).

To illustrate the effect of C_3, the simulated responses of the filter circuit model [see Fig. 6(b)] for various values of C_3 are shown in Fig. 8(a). Fig. 8(b) shows the curves to relate the transmission-zero frequencies to the values of C_3. As C_3 increases, the outer pair of transmission zeros will move toward the passband edges with the inner pair of transmission zeros essentially unchanged.

Note that an adjustment of the cross-coupling capacitance C_2 may alter both the locations of the inner and outer pairs of transmission zeros, as illustrated in Fig. 7(b), while an adjustment of the cross-coupling capacitance C_3 may only control the locations of the outer pair of transmission zeros, as demonstrated in Fig. 8(b). Therefore, a design guideline may be estab-
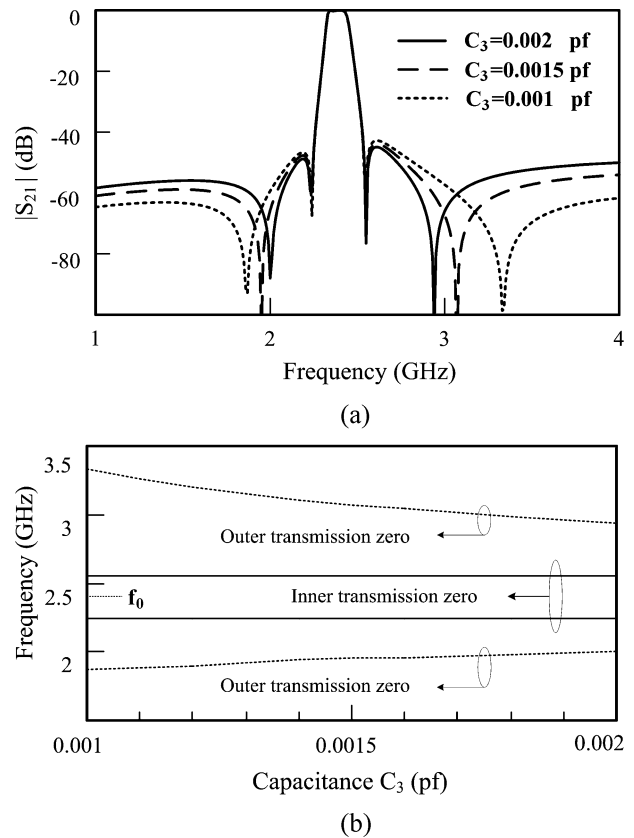
lished. Specifically, the cross-coupling capacitance C_2 is first selected to fulfill the selectivity requirement and the capacitance C_3 is then chosen to improve the stopband rejection. Since the cross-coupling capacitance C_3 essentially has no influence on the locations of the inner pair of the transmission zeros around the passband edge, this cross-coupling capacitance C_3 may thus be determined in the last step.

The design procedure for fourth-order filter may similarly be extended to the general nth filter ($n = $ even), again with the cross-coupling capacitance between input and output ports decided in the last step.

To demonstrate the adjustment of the locations of the upper and lower stopband transmission zeros, a full-wave simulation of the filter structure in Fig. 6(a) is conducted. Depicted in Fig. 9 are the corresponding simulated frequency responses, which show that the outer pair of transmission zeros can really be adjusted by varying the thickness d_1 [the gray portion of the metal in Fig. 6(a)] to change the value of C_3.

The proposed filter is designed according to the fourth-order maximally flat response with a center frequency of 2.39 GHz, a 3-dB bandwidth of 5.4%, and a reference impedance of 50 Ω. The required electrical length, capacitances C_1, C_1', and inductance L can be obtained based on the proposed equivalent-circuit model and filter synthesis formulas [1]. The corresponding geometrical parameters are also fine tuned in the full-wave simulator Ansoft Ensemble 8.0. The implemented filter is compact and has a dimension of $0.229\lambda \times 0.338\lambda$ ($l_3 = 17.4$ mm, $l_4 = 25.4$ mm).
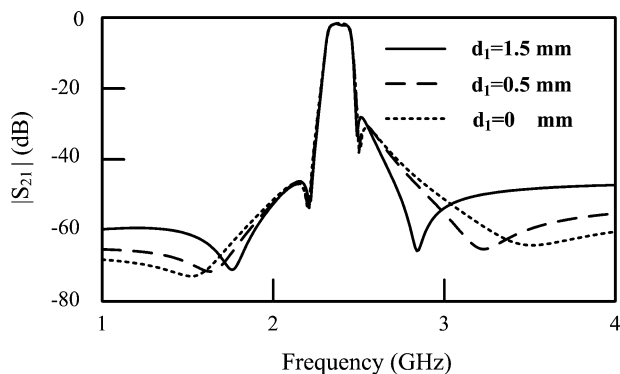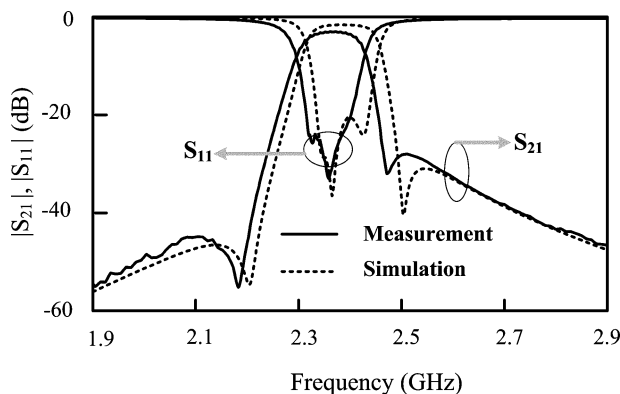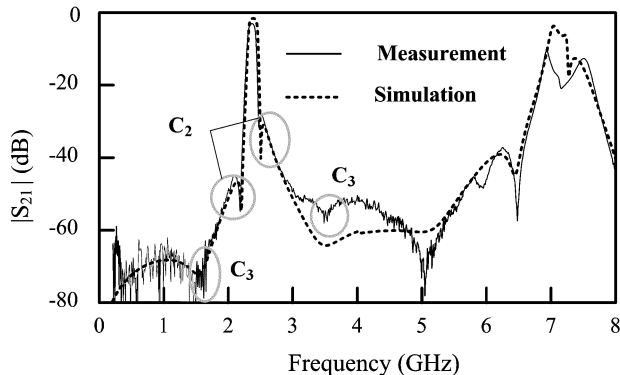
Fig. 9.   Full-wave simulated frequency responses of the fourth-order microstrip filter in Fig. 6(a) for various values of d_1.

(a)

(b)

Fig. 10.   Measured and simulated results of the proposed fourth-order microstrip filter in Fig. 6(a). (a) Narrow- and (b) wide-band frequency responses ($1_3 = 17.3$ mm, $1_4 = 27.3$ mm, $d_1 = 0$ mm).

The measured and simulated results for the implemented fourth-order microstrip filter [see Fig. 6(a)] are shown in Fig. 10. The measured center frequency is at 2.372 GHz, the minimum insertion loss is 2.95 dB at 2.372 GHz, and the 3-dB bandwidth is 5.2%. Good agreement between measured and simulated results is observed, except for a slight frequency shift of less than 1%. The two transmission zeros mainly decided by C_2 are located at 2.18 and 2.47 GHz and those by C_3 are located at 1.56 and 3.49 GHz. Note that no repeated passband at $2f_0$ is observed, as expected, and the stopband rejection is better than 45 dB below 2.2 GHz and from 2.86 ∼ 6.01 GHz. By a simple extension of the proposed fourth-order filter,

bandpass filters with higher order can also be implemented for better performance.

IV. CONCLUSIONS

In this study, compact second- and fourth-order microstrip bandpass filters have been proposed and carefully examined. By suitably introducing two capacitive cross-coupling paths in the fourth-order filter, two pairs of transmission zeros have been created. As a result, good selectivity and improved stopband rejection can be achieved simultaneously. The proposed filter structures also have the advantage of no repeated passband at twice the center frequency. Based on the proposed equivalent-circuit models, the design of the proposed filters is simple and may follow the conventional filter synthesis techniques. The locations of transmission zeros may easily be adjusted by varying the capacitances on the cross-coupling paths. In addition, the size of the proposed filters is much less than that of the conventional filters composed of $\lambda/4$ resonators. The proposed filters are useful for application in the communication system designs when both good selectivity and stopband rejection are required.

REFERENCES

[1]   G. L. Mattaei, L. Young, and E. M. T. Jones, *Microwave Filters, Impedance-Matching Networks, and Coupling Structures*.   Norwood, MA: Artech House, 1980.
[2]   E. G. Crystal and S. Frankel, "Hairpin-line and hybrid hairpin-line/half-wave parallel-coupled-line filters," *IEEE Trans. Microw. Theory Tech.*, vol. MTT-20, no. 11, pp. 719–728, Nov. 1972.
[3]   M. Sagawa, K. Takahashi, and M. Makimoto, "Miniaturized hairpin resonator filters and their application to receiver front-end MIC's," *IEEE Trans. Microw. Theory Tech.*, vol. 37, no. 12, pp. 1991–1997, Dec. 1989.
[4]   J. S. Hong and M. J. Lancaster, "Cross-coupled microstrip hairpin-resonator filters," *IEEE Trans. Microw. Theory Tech.*, vol. 46, no. 1, pp. 118–122, Jan. 1998.
[5]   J. T. Kuo, M. J. Maa, and P. H. Lu, "A microstrip elliptic function filter with compact miniaturized hairpin resonators," *IEEE Microw. Guided Wave Lett.*, vol. 10, no. 3, pp. 94–95, Mar. 2000.
[6]   C. M. Tsai, S. Y. Lee, and C. C. Tsai, "Performance of a planar filter using a 0° feed structure," *IEEE Trans. Microw. Theory Tech.*, vol. 50, no. 10, pp. 2362–2367, Oct. 2002.
[7]   G. L. Matthaei, "Interdigital bandpass filters," *IEEE Trans. Microw. Theory Tech.*, vol. MTT-10, no. 11, pp. 479–491, Nov. 1962.
[8]   M. Dishal, "A simple design procedure for small percentage bandwidth round-rod interdigital filters," *IEEE Trans. Microw. Theory Tech.*, vol. MTT-13, no. 11, pp. 696–698, Nov. 1965.
[9]   E. G. Cristal, "Tapped-line coupled transmission lines with applications to interdigital and combline filters," *IEEE Trans. Microw. Theory Tech.*, vol. MTT-23, no. 12, pp. 1007–1012, Dec. 1975.
[10]   C. Y. Chang, C. C. Chen, and H. J. Huang, "Folded quarter-wave resonator filters with Chebyshev, flat group delay, or quasi-elliptical function response," in *IEEE MTT-S Int. Microw. Symp. Dig.*, Seattle, WA, Jun. 2002, pp. 1609–1612.
[11]   C. Y. Chang and C. C. Chen, "A novel coupling structure suitable for cross-coupled filters with folded quarter-wave resonators," *IEEE Microw. Wireless Compon. Lett.*, vol. 13, no. 12, pp. 517–519, Dec. 2003.
[12]   C. C. Chen, Y. R. Chen, and C. Y. Chang, "Miniaturized microstrip cross-coupled filters using quarter-wave or quasi-quarter-wave resonators," *IEEE Trans. Microw. Theory Tech.*, vol. 51, no. 1, pp. 120–131, Jan. 2003.
[13]   H. K. Pang, K. M. Ho, K. W. Tam, and R. P. Martins, "A compact microstrip $\lambda/4$-SIR interdigital bandpass filter with extended stopband," in *IEEE MTT-S Int. Microw. Symp. Dig.*, Fort Worth, TX, Jun. 2004, pp. 1621–1624.
[14]   P. H. Deng, C. H. Wang, Y. S. Lin, and C. H. Chen, "A novel compact microstrip bandpass filter with two transmission zeros," in *Proc. 34th Microw. Eur. Conf.*, Amsterdam, The Netherlands, Oct. 2004, pp. 633–636.
[15]   R. Levy and J. D. Rhodes, "A comb-line elliptic filter," *IEEE Trans. Microw. Theory Tech.*, vol. 19, no. 1, pp. 26–29, Jan. 1971.

Pu-Hua Deng was born in Kaohsiung, Taiwan, R.O.C., in 1978. He received the B.S. degree in electrical engineering from National Sun Yet-Sen University, Kaohsiung, Taiwan, R.O.C., in 2002, the M.S.E.E. degree from National Taiwan University, Taipei, Taiwan, R.O.C., in 2004, and is currently working toward the Ph.D. degree at National Taiwan University.

His research interests include the design and analysis of microwave filter circuits.

Chi-Hsueh Wang was born in Kaohsiung, Taiwan, R.O.C., in 1976. He received the B.S. degree in electrical engineering from National Cheng Kung University, Tainan, Taiwan, R.O.C., in 1997, and the Ph.D. degree from National Taiwan University, Taipei, Taiwan, R.O.C. in 2003.

He is currently a Post-Doctoral Research Fellow with the Graduate Institute of Communication Engineering, National Taiwan University. His research interests include the design and analysis of microwave and millimeter-wave circuits and computational electromagnetics.

Yo-Shen Lin (M'04) was born in Taipei, Taiwan, R.O.C., in 1973. He received the B.S. and M.S.E.E. degrees in electrical engineering and Ph.D. degree in communication engineering from National Taiwan University, Taipei, Taiwan, R.O.C., in 1996, 1998, and 2003, respectively.

From 1998 to 2001, he was an RF Engineer with Acer Communication and Multimedia Inc., Taipei, Taiwan, R.O.C., where he designed global system for mobile communication (GSM) mobile phones. From 2001 to 2003, he was with Chi-Mei Communication System Inc., Taipei, Taiwan, R.O.C. where he was involved with the design of low-temperature co-fired ceramic (LTCC) RF transceiver modules for global system for mobile communications (GSM) mobile applications. In August 2003, he joined the Graduate Institute of Communication Engineering, National Taiwan University, as a Post-Doctoral Research Fellow, and became an Assistant Professor in August 2004. Since August 2005, he has been with the Department of Electrical Engineering, National Central University, Chungli, Taiwan, R.O.C., where he is currently an Assistant Professor. His research interests include the design and analysis of miniature planar microwave circuits and RF transceiver module for wireless communication systems.

Dr. Lin was the recipient of the Best Paper Award of the 2001 Asia–Pacific Microwave Conference (APMC), Taipei, Taiwan, R.O.C., and the 2005 Young Scientist Award presented at the URSI General Assembly, New Delhi, India.

Chun Hsiung Chen (SM'88–F'96) was born in Taipei, Taiwan, R.O.C., on March 7, 1937. He received the B.S.E.E. and Ph.D. degrees in electrical engineering from National Taiwan University, Taipei, Taiwan, R.O.C., in 1960 and 1972, respectively, and the M.S.E.E. degree from National Chiao Tung University, Hsinchu, Taiwan, R.O.C., in 1962.

In 1963, he joined the Faculty of the Department of Electrical Engineering, National Taiwan University, where he is currently a Professor. From August 1982 to July 1985, he was Chairman of the Department of Electrical Engineering, National Taiwan University. From August 1992 to July 1996, he was the Director of the University Computer Center, National Taiwan University. In 1974, he was a Visiting Scholar with the Department of Electrical Engineering and Computer Sciences, University of California at Berkeley. From August 1986 to July 1987, he was a Visiting Professor with the Department of Electrical Engineering, University of Houston, TX. In 1989, 1990, and 1994, he visited the Microwave Department, Technical University of Munich, Munich, Germany, the Laboratoire d'Optique Electromagnetique, Faculte des Sciences et Techniques de Saint-Jerome, Universite d'Aix-Marseille III, Marseille, France, and the Department of Electrical Engineering, Michigan State University, East Lansing, respectively. His areas of interest include microwave circuit analysis and computational electromagnetics.